

Tradeoff Analysis of Aerodynamic Wing Design for RLV

K. Chiba^a, S. Obayashi^a and K. Nakahashi^b

^aInstitute of Fluid Science, Tohoku University,
Katahira 2-1-1, Aoba-ku, Sendai 980-8577, Japan

^bDepartment of Aeronautics and Space Engineering, Tohoku University,
Aramaki-aza-aoba 6-6-01, Aoba-ku, Sendai 980-8579, Japan

The wing shape of flyback booster for a Two-Stage-To-Orbit reusable launch vehicle has been optimized considering four objectives. The objectives are to minimize the shift of aerodynamic center between supersonic and transonic conditions, transonic pitching moment and transonic drag coefficient, as well as to maximize subsonic lift coefficient. The three-dimensional Reynolds-averaged Navier-Stokes computation using the modified Spalart-Allmaras one-equation model is used in aerodynamic evaluation accounting for possible flow separations. Adaptive range multi-objective genetic algorithm is used for the present study because tradeoff can be obtained using a smaller number of individuals than conventional multi-objective genetic algorithms. Consequently, four-objective optimization has produced 102 non-dominated solutions, which represent tradeoff information among four objective functions. Moreover, Self-Organizing Maps have been used to analyze the present non-dominated solutions and to visualize tradeoffs and influence of design variables to the four objectives. Self-Organizing Maps contoured by the four objective functions and design variables are found to visualize tradeoffs and effects of each design variable.

Key Words: Aerodynamic Flow, Optimization Problems

1. Introduction

Space transportation system with a substantial cost reduction needs to be proposed so that space utilization in many disciplines is performed more actively. For its manner, the research was focused on the reusable launch vehicle (RLV) system[1]. RLV is suggested instead of the present expendable launch vehicle (ELV) system, and many research for RLV is performed. Especially, Single-Stage-To-Orbit (SSTO) launch system, for example, X-33, was studied by many researchers[2] because this configuration was ideal for reuse similar to airplane. However, it was found through those researches that SSTO configuration had difficulties because it would require higher performance propulsion system and larger reduction of its structure weight than those based on the present technology. Consequently, current proposals for the introduction of reusable components in space transportation regard Two-Stage-To-Orbit (TSTO) configuration with winged flyback booster powered by liquid rocket engines[3] for vertical-take off-horizontal-landing

(VTHL). For the realization of this configuration, many approaches are performed from design variation, system achievement, materials, structure weight, control, and trajectory analysis, *etc.* Considering the detailed aerodynamic performance[4], however, the shape design concept was not mentioned clearly. There is no concrete design precept about winged flyback booster.

As space transport system has more severe flight conditions than the existent airplane, the geometry of winged flyback booster is highly constrained, especially the wing has severe shape constraints. Nevertheless, the wing is the most important element for flyback booster because it generates the aerodynamic performance to fly-back. Therefore, each relationship among aerodynamic characteristics as lift, drag and moment becomes significant design information. Moreover, it is important that the sensitive design variables to the aerodynamic performance are found, namely, the acquisition of the knowledge about the design space is essential so that the aerodynamic performance of winged flyback booster is improved under severe shape constraints.

In the present study, the wing shape of TSTO RLV flyback booster has been optimized with the four objectives about aerodynamic performance. From the optimization results, tradeoff analysis has been performed among the four objectives. By using a data mining technique, the design knowledge has been obtained considering TSTO RLV winged flyback booster.

2. Multi-Objective Aerodynamic Optimization

2.1. Problem Definition

The reference mission of the TSTO RLV is to transport a 10t payload into low earth orbit (LEO), similar to the present mission of H-IIA. Due to a preliminary computation through the empirical equations developed by Japan Aerospace Exploration Agency (JAXA), the booster sizing is obtained. Among the calculated geometrical data, the minimum fuselage diameter and the fuselage length are employed as constraints in the present optimization. This means that the fuselage geometry is fixed to the given size and only the wing shape is allowed to be optimized in the present parameterization system. The main reason for keeping the fuselage geometry fixed is that the fuselage is filled with the liquid propellant rocket engines, so its size can hardly be changed.

The trajectory analysis[5] around a typical TSTO configuration based on the present mission shows that the separation of the booster and orbiter takes place roughly at Mach number of 3, altitude of 30,000m. Then, the flyback booster turns over, slows down, cruises at transonic speeds and lands at a subsonic speed. Note that the major part of its crossrange is in the transonic region. In the present study, the following four objective functions are considered:

Obj. 1: Minimization of the shift of the aerodynamic center between supersonic and transonic flights,

$$F_1 = |C_{M_p}^{\text{supersonic}} - C_{M_p}^{\text{transonic}}| \quad (1)$$

A significant control problem related to the RLV flight may originate in a large variation of the aerodynamic center between supersonic and transonic flight conditions. It is, then, desirable to design wing shapes with a less variation in the aerodynamic center. It will yield easier stability control.

Obj. 2: Minimization of the pitching moment at the transonic flight conditions,

$$F_2 = |C_{M_p}^{\text{transonic}}| \quad (2)$$

It is known that the arrow wing ensures high aerodynamic performance, while it also produces a large pitching moment. Thus, it should be minimized at the transonic flight conditions for less trim drag and better flight stability.

Obj. 3: Minimization of the drag at the transonic flight conditions,

$$F_3 = C_D^{\text{transonic}} \quad (3)$$

The trajectory analysis shows that the range of RLV booster is mostly covered by the transonic flight. Thus, the transonic drag should be minimized to increase the flight range.

Obj. 4: Maximization of the lift at the subsonic flight conditions,

$$F_4 = C_L^{\text{subsonic}} \quad (4)$$

To reduce the required runway distance, the lift obtained at the subsonic flight conditions should be maximized.

2.2. Optimizer

Adaptive range multi-objective genetic algorithm (ARMOGA)[6] is an efficient multi-objective evolutionary algorithm (MOEA) designed for aerodynamic optimization and multidisciplinary design optimization problems using high-fidelity CFD solvers with a large computational time. ARMOGA has the range adaptation based on population statistics, thus the population is re-initialized at every N generations so that the search region adapts toward promising regions.

2.3. Aerodynamic Evaluation

In the present study, the unstructured mesh method[7,8] is used to evaluate aerodynamic performance. The three-dimensional Reynolds-averaged Navier-Stokes (RANS) equations are computed with a finite-volume cell-vertex scheme. The unstructured hybrid mesh method[9] is applied to capture the boundary layer accurately and efficiently. The Harten-Lax-van Leer-Einfeldt-Wada Riemann solver[10] is used for the numerical flux computations. The Venkatakrishnan's limiter[11] is applied when reconstructing second order accuracy. The lower-upper symmetric-Gauss-Seidel implicit scheme[12] is applied for time integration. Considering a turbulence model, the Spalart-Allmaras one-equation model modified by Dacles-Mariani *et al.*[13] is employed without transition.

Three RANS computations per candidate solution are carried out, at three instances of the vehicle trajectory, at supersonic, transonic and subsonic flow conditions. Taking advantage of the parallel search in EAs, the present optimization is parallelized on vector-parallel machines NEC SX-5. The master processing element (PE) manages ARMOGA, while the slave PEs compute CFD processes. Slave processes do not require synchronization.

2.4. Geometry Definition

The design variables are related to planform, airfoil shapes, wing twist and relative position to fuselage[6]. A wing planform is determined by five design variables as shown

in Fig. 1. A kink is placed on the leading edge. Airfoil shapes are defined at wing root, kink and tip, respectively, using thickness distributions and camber lines. The thickness distributions are described by Bézier curves using eleven control points and linearly interpolated in the spanwise direction. The camber line distributions are parameterized using Bézier curves with four control points, respectively, and linearly incorporated in the spanwise direction. Wing twist is refined using B-splines with six control points. Relative position of the wing root to the fuselage is parameterized by x and z coordinates of the leading edge, angle of attack and dihedral angle. An entire wing shape is thus defined by using 71 design variables. Once a wing is defined, a junction line between wing and fuselage is extracted and, by neglecting a part of wing inside fuselage, the final wing-fuselage geometry is derived[14].

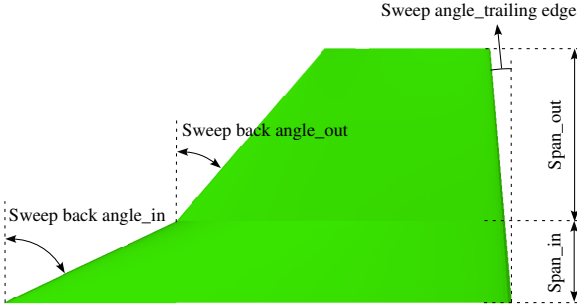


Figure 1. Wing planform shape definition along with some of the major design parameters.

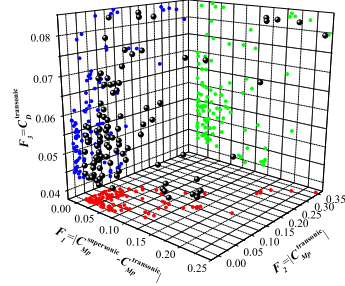


Figure 2. Derived non-dominated solutions plotted in the (F_1, F_2, F_3) objective functions three dimensional space.

3. Optimization Results

As the population size is set to eight, the CFD preprocesses are parallelized on eight PEs. Because a design candidate has to be evaluated at the three flow conditions which are summarized in Table 1, 24 RANS computations are needed in one generation. The population is re-initialized at every five generations for the range adaptation. The total evolutionary computation of 40 generations is performed. Consequently, the total 102 non-dominated solutions are obtained for tradeoff analysis.

Figure 2 shows the resulting non-dominated solutions projected onto the three-dimensional objective function space for the first three objectives. And Figure 3 shows the four two-dimensional projections of the non-dominated solutions to understand tradeoffs among the four objective functions better.

Table 1

Flow conditions for the three Navier-Stokes computations.

| <i>Flying Condition</i> | M | AoA | Re |
|-------------------------|-----|-------|-----------------|
| Supersonic flight | 1.2 | 0.0 | 6×10^6 |
| Transonic flight | 0.8 | 8.0 | 6×10^6 |
| Subsonic flight | 0.3 | 13.0 | 6×10^7 |

The optimum values of F_1 and F_2 are zero, the non-dominated solutions attain the origin, namely the optimum values of F_1 and F_2 in Fig. 3(a). As the plots in Fig. 3(a) are the non-dominated solutions for not two objective functions but four objective functions, there is a tradeoff surface spread of that the non-dominated solutions near the origin. Figure 3(a) shows there is no tradeoff between the shift of aerodynamic center and the transonic pitching moment.

The Pareto front for F_2 attains the optimum front, however, the Pareto front for F_3 does not reach C_D of 0 obviously in Fig. 3(b). Thus, Figure 3(b) shows there is a slight tradeoff between F_2 and F_3 , the transonic drag can be improved while the transonic pitching moment decreases.

The Pareto front is clearly shown between F_3 and F_4 in Fig. 3(c). Thus, Figure 3(c) indicates there is a severe tradeoff between the transonic drag and the subsonic lift. This result inspires high lift device may be needed for RLV booster for landing, similar to aircraft.

Figure 3(d) shows the same situation of Fig. 3(b), the Pareto front for F_1 attains the optimum front, however, the Pareto front for F_4 does not have an apparent limit. Therefore, Figure 3(d) shows there is a slight tradeoff between F_1 and F_4 . This indicates the shift and the transonic pitching moment optimized simultaneously while the subsonic lift increases slightly.

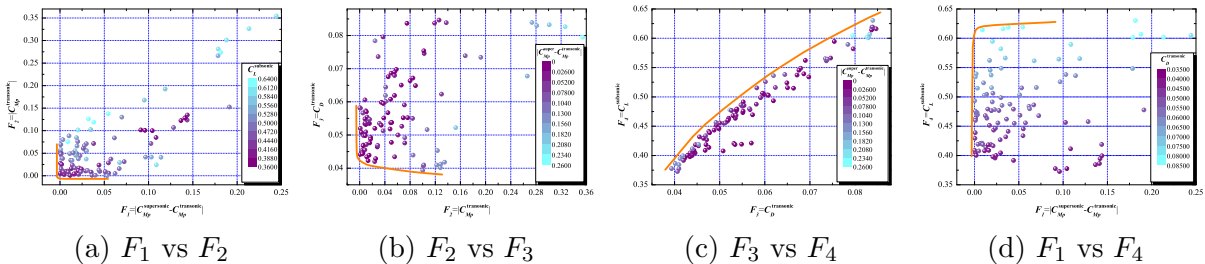


Figure 3. Derived non-dominated solutions on two dimensional plane between two objectives.

4. Data Mining by Self-Organizing Map

If the optimization problem has only two or three objectives, tradeoffs can be visualized easily. However, if there are more than four objectives, the technique to visualize the computed non-dominated solutions is needed. Therefore, in the present study, Self-Organizing Maps (SOMs) suggested by Kohonen[15] have been employed. SOM is not only the technique for the visualization but also the application tool for the intelligent compression of the information. In other words, SOM can be applied for the data mining technique to acquire the knowledge about design space. In this study, Viscovery[®] SOMine produced by Eudaptics GmbH in Austria is employed(See Ref. 16 for more details).

4.1. Visualization of Design Tradeoffs

The resulting 102 non-dominated solutions have been projected onto the two-dimensional map of SOM. Figure 4 shows the resulting SOM with 10 clusters considering the four objectives. Furthermore, Figure 5 shows the SOMs colored by the four objective values, respectively. This color figures show the SOM in Fig. 4 can be grouped as follows: Upper

center area in Fig. 4 corresponds to the designs with the low shift of aerodynamic center. Upper right corner corresponds to the designs with the low shift of aerodynamic center, transonic pitching moment and transonic drag. Lower right corner corresponds to the designs with the low transonic drag. Lower left corner corresponds to the high shift of aerodynamic center, transonic pitching moment and transonic drag. Left center region corresponds to the high subsonic lift.

In addition, Figures 5(a) and 5(b) show high value regions for the shift of aerodynamic center and the transonic drag coincide with each other. As Figure 5(c) is very similar to Fig. 5(d), severe tradeoff exists between the transonic drag and the subsonic lift because the transonic drag is to be minimized and the subsonic lift is to be maximized.

4.2. Data Mining of Design Space

The SOM as Fig. 4 can be contoured by 71 design-variable values. Especially, four characteristic design variables will be considered here.

Figure 6(a) shows the SOM colored by the design variable of x coordinate of wing position to fuselage illustrated in Fig. 6(b). Here, x coordinate is held on the fuselage. Higher value exists on the lower left corner in Figs. 5(a) and 5(b). This area is a cluster of high values of the shift of aerodynamic centers, transonic pitching moment and transonic drag. Thus, this means that the values of shift, transonic pitching moment and transonic drag become worse when the wing position is backward of fuselage.

Figure 7(a) shows the SOM colored by the design variable of rearward camber height at the wing tip illustrated in Fig. 7(b). Lower values exist on the right side in Fig. 5(c) which shows the SOM colored by the transonic drag coefficient. This area is a cluster of low value of transonic drag in Fig. 4. Thus, Fig. 7(a) means a individual with lower rearward camber height at the wing tip has lower transonic drag.

Figure 8(a) shows the SOM colored by the design value of the rearward camber height at the kink illustrated in Fig. 8(b). Higher values exist on the left side in Fig. 5(d) which shows the SOM colored by the subsonic lift coefficient. Hence, Fig. 8(a) means a individual with higher rearward camber height at the kink has higher subsonic lift.

Finally, Fig. 9 shows the SOM colored by several other design variables. As these maps have incoherent coloring, these design variables have no effects of determining tradeoffs among four objectives.

5. Conclusion

The wing for a TSTO RLV flyback booster powered by liquid propellant rocket engine for VTHL has been optimized considering four aerodynamic objective functions using ARMOGA. Consequently, the tradeoff information among four objective functions has been revealed. No tradeoff exists between the shift of aerodynamic center and transonic pitching moment. Severe tradeoff exists between transonic drag and subsonic lift. Slight tradeoffs exist between other combinations of objectives.

Moreover, data mining for the design space has been performed using SOM. For example, wing position should not be so backward to fuselage to decrease of shift of aerodynamic center between supersonic and transonic flow conditions, transonic pitching moment and transonic drag. Rearward camber height at tip has an influence to reduce/increase transonic drag. Rearward camber height at kink has an influence to increase subsonic lift.

Strake has less effect to subsonic lift increase and the primary leading-edge separation from the outboard wing is more important for vortex lift. Data mining provides knowledge about the design space, which is considered an important facet of solving optimization problems.



Figure 4. SOM of the non-dominated solutions in the four dimensional objective function space.

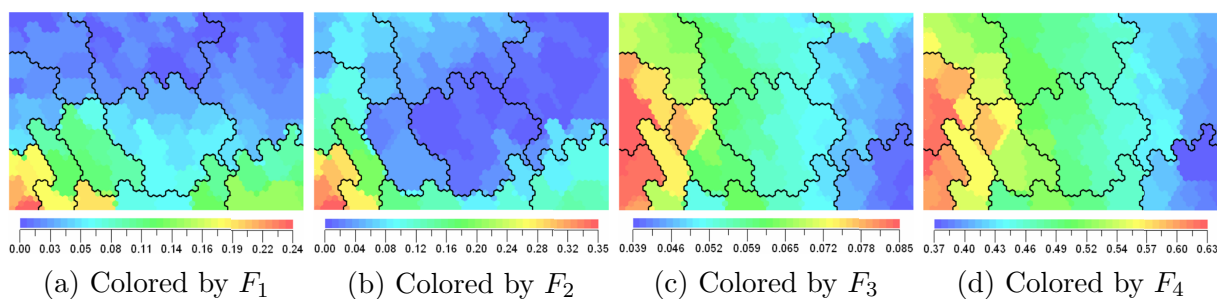


Figure 5. SOM colored by the objective functions.

REFERENCES

1. R. W. Powell, M. K. Lockwood, and S. A. Cook. The Road from the NASA Access-to-Space Study to a Reusable Launch Vehicle. IAF-98-V.4.02, 1998, 1998.
2. A. W. Wilhite, L. B. Bush, C. I. Cruz, R. A. Lepsh, W. D. Morris, D. O. Stanley, and K. E. Wurster. Advanced Technologies for Rocket Single-Stage-to-Orbit Vehicles. *Journal of Spacecraft*, Vol. 28, No. 6, pp. 646–651, 1991.
3. M. Sippel, A. Herbertz, J. Kauffmann, and V. Schmid. Analysis of liquid fly-back booster performance. AIAA Paper 99-4827, 1999, 1999.
4. B. N. Pamadi, G. J. Brauckmann, M. J. Rush, and H. D. Fuhrmann. Aerodynamic Characteristics, Database Development and Flight Simulation of the X-34 Vehicle. AIAA Paper 2000-0900, 2000, 2000.
5. T. Iwata, K. Sawada, and K. Kamijo. Conceptual Study of Rocket Powerd TSTO with Fly-back Booster. AIAA Paper 2003-4813, 2003, 2003.
6. D. Sasaki, S. Obayashi, and K. Nakahashi. Navier-Stokes Optimization of Supersonic Wings with Four Objectives Using Evolutionary Algorithm. *Journal of Aircraft*, Vol. 39, No. 4, pp. 621–629, 2002.
7. Y. Ito and K. Nakahashi. Direct surface triangulation using stereolithography data. *AIAA Journal*, Vol. 40, No. 3, pp. 490–496, 2002.
8. D. Sharov and K. Nakahashi. A Boundary Recovery Algorithm for Delaunay Tetrahedral Meshing. In *Proceedings of the 5th International Conference on Numerical Grid Generation in Computational Field Simulations*, pp. 229–238, 1996.

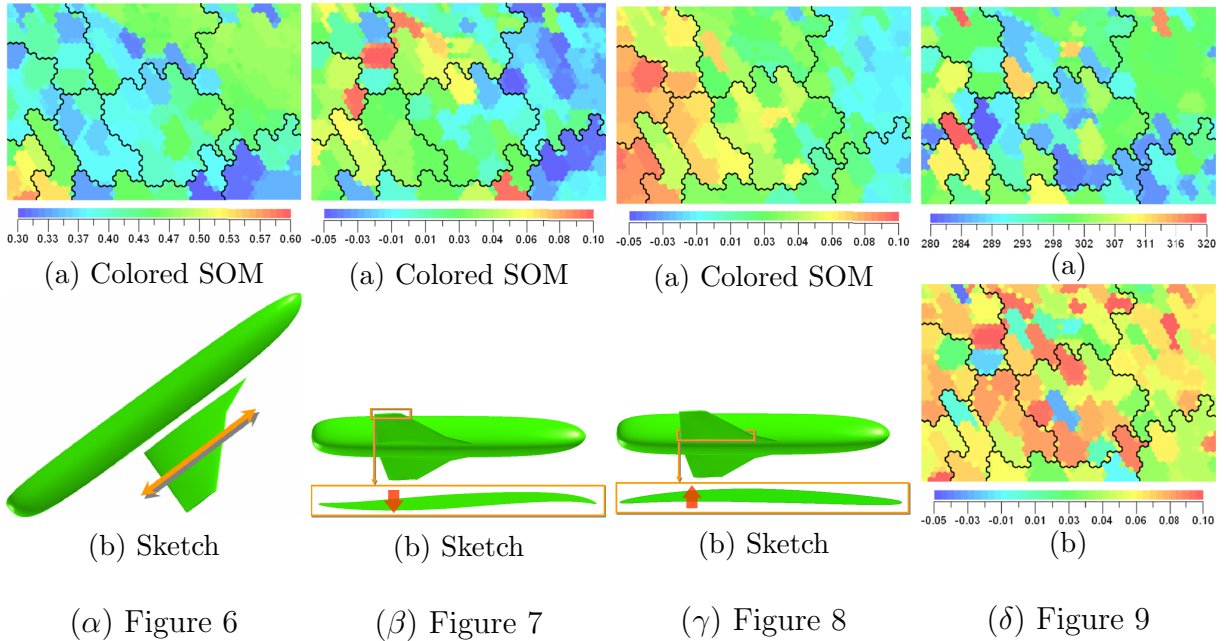


Figure 6. Design variable of x coordinate of wing position to fuselage.

Figure 7. Design variable of rearward camber height at the wing tip.

Figure 8. Design variable of rearward camber height at the kink.

Figure 9. Several design variables with no relation to the objective functions. (a) SOM colored by the design variable of relative size between wing and fuselage. (b) SOM colored by the design variable of frontward camber height at the kink.

9. Y. Ito and K. Nakahashi. Improvements in the Reliability and Quality of Unstructured Hybrid Mesh Generation. In *International Journal for Numerical Methods in Fluids*, pp. 79–108, Vol. 45, Issue 1, 2004.
10. S. Obayashi and G. P. Guruswamy. Convergence Acceleration of an Aeroelastic Navier-Stokes Solver. *AIAA Journal*, Vol. 33, No. 6, pp. 1134–1141, 1994.
11. V. Venkatakrishnan. On the Accuracy of Limiters and Convergence to Steady State Solutions. AIAA Paper 93-0880, 1993, 1993.
12. D. Sharov and K. Nakahashi. Reordering of Hybrid Unstructured Grids for Lower-Upper Symmetric Gauss-Seidel Computations. *AIAA Journal*, Vol. 36, No. 3, pp. 484–486, 1998.
13. J. Dacles-Mariani, G. G. Zilliac, J. S. Chow, and P. Bradshaw. Numerical/Experimental Study of a Wingtip Vortex in the Near Field. *AIAA Journal*, Vol. 33, No. 9, pp. 1561–1568, 1995.
14. D. Sasaki, G. Yang, and S. Obayashi. Automated Aerodynamic Optimization System for SST Wing-Body Configuration. *Transactions of the Japan Society for Aeronautical and Space Sciences*, Vol. 46, No. 154, pp. 230–237, 2004.
15. T. Kohonen. *Self-Organizing Maps*. Springer, Berlin, Heidelberg, 1995.
16. G. Deboeck and T. Kohonen. *Visual Explorations in Finance with Self-Organizing Maps*. London, Springer Finance, 1998.